Proceedings of the 4th International Conference on Biological Engineering and Medical Science
DOI: 10.54254/2753-8818/59/20241388

Exploring the interactions between peritoneal dendritic cells and T cells: Implications for cancer metastasis

Bolin Miao

Dana Hall School, MA, USA

bolin.miao@danahall.org

Abstract. Ovarian Cancer (OC) is a formidable challenge as a gynecological malignancy with ascites, the abnormal accumulation of fluid in the peritoneal cavity, serving as a clinical hallmark of advancement and metastasis. While OC immune analyses focus on solid tumors, little is known about malignant ascites inhabitants during peritoneal metastasis. Here, we focused on a single-cell landscape of the OC ecosystem in malignant ascites with comparison to tumor sites. Our data analysis reveals that compared to the immunosuppressed tumor, ascites contained less exhausted, more memory-like T cells, which correlated with prolonged survival in stages III/IV OC. Furthermore, we characterized the substantial interactions between dendritic cells and T cells. Lastly, an in vitro dendritic cell culture system from blood cells for potential novel cancer vaccine design was explored. Taken together, this study reveals T cell memory and effector potential amidst immunosuppressive pressures in ascites and provides valuable insight into the cross-talk between dendritic cells and T cells that potentially contributes to the unique T cell profile in the ascites ecosystem.

Keywords: Ovarian Cancer (OC), prognosis, cancer vaccine, malignant ascites, dendritic cells, T cells.

1. Introduction

Ovarian cancer (OC) is the most lethal gynecological malignancy and has a leading incidence rate of 6.6% across both sexes [1]. It is the seventh leading cause of cancer mortality in women worldwide, accounting for 5% of cancer deaths in females. OC is a heterogeneous disease and High-grade serous ovarian cancer (HGSOC) stands out as the predominant histological subtype among all ovarian cancer types, encompassing over 70% of ovarian cancer patients [1]. Following diagnosis, more than 75% of HGSOC patients exhibit an advanced stage of the disease characterized by extensive metastasis and the presence of ascites. Notably, patients with peritoneal metastasis have a significantly worse prognosis than those with other isolated sites of metastases. Though advanced chemo- and targeted-therapy has been developed, the 5-year relative survival rate for metastatic OC patients is still lower than 20% [2]. In the past decade, immune checkpoint blockade (ICB) has achieved great success in treating metastatic melanoma and non-small cell lung cancer (NSCLC) with more than half of the patients' survival over 5 years [3]. However, gynecological malignancies minimally respond to current ICB due to a lack of fundamental understanding of the heterogeneous tumor-intrinsic and tumor-extrinsic immunotherapy-resistant mechanisms in metastatic diseases [4].

DOI: 10.54254/2753-8818/59/20241388

The peritoneal cavity is a space filled with fluid that accommodates the majority of abdominal organs. Peritoneal mesothelial cells secrete surfactants that lubricate peritoneal organs as well as enzymes and signaling molecules that control the function of hemapoietic cells present in the peritoneal cavity [5]. Therefore, the peritoneal fluid is not only important for organ lubrication but also holds a comprehensive ecosystem of immune cells including B cells, T cells, and myeloid cells such as dendritic cells and macrophages.

Previous studies focused on immune cells inside the tumor, ignoring the interactions and function of peritoneal immune cells surrounding the tumor, in ascites, during cancer progression and peritoneal metastasis. Among these understudied peritoneal immune cells, T cells most directly interact with tumor cells. Upon activation, Naive CD8+ T cells undergo differentiation into various types, including Stem Cell Memory cells (Tscm), Central Memory cells (Tcm), Effector Memory cells (Tem), and Effector cells (Teff), ordered based on effector function. Notably, their cytotoxicity can be suppressed as they undergo exhaustion under overexpression of co-inhibitory receptors (e.g. CTLA4 and PD1) and chronic antigen stimulation [6]. CD4+ cells display helper functions to other groups of cells such as Cytotoxic T cells and B cells, further differentiating into distinct subsets, including Th1, Th2, Th9, Th17, Th22, Treg (regulatory T cells), and Tfh (follicular helper T cells). Notably, FOXP3+ Tregs display immunosuppressive properties, crucial for preventing excessive immune responses that could lead to autoimmunity or tissue damage [7]. In addition to T cells, the peritoneal cavity contains myeloid cells with a majority population of macrophage and dendritic cells (DC). DCs are generally divided into XCR1+CD103+ conventional DC1 (cDC1) and CD1c+CD11c+ cDC2. cDC1 performs antigen cross-presentation required to prime CD8 T cells while cDC2 is specialized in priming CD4+ T cells. A third population of subset of CD1c+CD14+ monocyte-derived dendritic cells (moDC), emerging in the context of pathogenic inflammation, exhibits a hybrid phenotype of both monocytes and dendritic cells. This subset demonstrates the capacity to reactivate effector and memory T cells [8].

Limited studies have explored the peritoneal immune cell landscape. For example, GZMK+ memory T cells in ascites were identified as a potential origin for tumor-infiltrating T cells. The heterogeneity of macrophages was characterized, distinguishing between the roles of tumor-associated macrophages (TeMs) and ascites-enriched macrophages (AeMs) in immune regulation and inflammation [9]. Research has also touched on dendritic cell subsets, claiming cDC2's predominance in the omentum and proliferation in ascites of nonresponsive patients [9].

Despite advancements in understanding the immune landscape of peritoneal malignancies, several critical questions remain unanswered. In particular, comprehensive side-by-side analyses of T cell phenotypes in ascites versus in tumors are lacking. Elucidating ascites T cell biology, especially myeloid-T cell interactions governing this niche, emerges as an area of scientific interest. Moreover, the comparison of normal peritoneal immune responses with those observed in the metastatic setting remains an understudied aspect. Notably, the clinical significance of ascites as a prognostic indicator in High-Grade Serous Ovarian Cancer (HGSOC) [9] emphasizes the urgency to delve into the functional dynamics of peritoneal immune cells during cancer progression. This project aims to bridge these knowledge gaps by employing a multifaceted approach. Through computational analyses and experimental investigations, we seek to decipher phenotypic disparities among T cells in blood, ascites, and tumors. Additionally, we aim to unravel the interactions between peritoneal immune cells, particularly dendritic cells, and T cells, shedding light on their potential roles in peritoneal cancer progression. We also explored an *in vitro* dendritic cell culture system from blood cells for potential novel cancer vaccine design.

2. Methods

2.1. Data collection

Raw gene expression profiles for the single cell RNA-seq data for the ascites and tumor from ovarian cancer patients were downloaded from https://doi.org/10.17632/rc47y6m9mp.1

DOI: 10.54254/2753-8818/59/20241388

Raw gene expression profiles for the single cell RNA-seq data for the peritoneal wash from healthy donors were accessed via GEO with accession number GSE228030.

2.2. scRNA-seq data preprocessing

The UMI counts-based gene expression matrix was processed using the R package Seurat (v5). To exclude low-quality cells, those with less than 200 genes detected, or more than 10% mitochondrial genes, were filtered from the dataset. To remove potential multiplets, cells with a total number of UMI counts higher than 50,000 or a number of genes detected higher than 6,000 were also removed. The number of UMIs of all cells in each sample was first log-normalized and the highly variable features were identified. Harmony integration was then performed. This method has been shown to both robustly correct for technical differences between datasets (i.e. batch effect correction), and to perform comparative scRNA-seq analysis of across experimental conditions. Principle component (PC) analysis was then performed over the integrated dataset and clusters were identified using k-nearest-neighbor graph-based clustering, implemented in the R functions FindNeighbors and FindClusters, on the basis of the first 25 PCs. The same PCs were used to generate the uniform manifold approximation and projection (UMAP) projections for visualization.

2.3. Identification of marker genes for each cluster

Upregulated biomarker genes for each cluster were identified by analyzing differentially expressed genes relative to all other clusters, using the Wilcoxon rank sum test embedded in the function FindAllMarkers of the R package Seurat. P values were corrected for multiple comparisons by the Bonferroni method. Genes with a log2 fold-change (log2FC) > 0.25 and adjusted P value < 0.05 were considered cluster-specific marker genes.

2.4. Gene set enrichment analysis (GSEA)

We first defined comprehensive gene signatures for all CD8+ T cells in ascites versus in tumor as well as the gene signatures of each cluster identified by a two-way wilcox test, corrected for multiple comparisons by the Benjamini–Hochberg procedure. Adjusted P values less than 0.05 and average log2-fold gene expression change higher than 0.5 were used as the cutoffs to generate the gene signature. Both signatures were added to the 'c2.all.v6.2.symbols' gene sets collection from the MSigDB database (modified C2 dataset) for GSEA analysis. We then performed preranked GSEA using the GSEA_4.0.3 software on the clusters of interest from the scRNA-seq analysis using the log2FC as the ranking metric for preranked GSEA.

2.5. Survival analysis

Associations between gene expression and overall survival of ovarian cancer patients were analyzed using the web based tool "KM Plotter" (http://kmplot.com) with the following settings: "auto select best cutoff," probe set option: "JetSet best probe," histology: all, datasets: all; stage: stageIII-IV, other settings: default). The 2015 version of KM Plotter used contains the following 13 datasets: GSE14764 (n = 80), GSE15622 (n = 36), GSE18520 (n = 63), GSE19829 (n = 28), GSE23554 (n = 28), GSE26193 (n = 107), GSE26712 (n = 195), GSE27651 (n = 49), GSE30161 (n = 58), GSE3149 (n = 116), GSE51373 (n = 28), GSE9891 (n = 285), TCGA (n = 565). A total of 487 patients matched the selection criteria and were used for survival analysis. The average z-transformed expression values of the top 100 genes from each cluster were used to generate scores, and Cox proportional hazard models were used to determine the association between each cluster-specific score and patient overall survival. Patient samples were dichotomized into two groups using the median score as the cutoff. A univariate Cox regression model was used to determine the association between each dichotomized score and patient survival.

DOI: 10.54254/2753-8818/59/20241388

2.6. NicheNet analysis

We defined a list of candidate ligands and receptors based on their known biological functions and expression patterns observed in our scRNA-seq dataset. By applying NicheNet's algorithm, we quantitatively ranked these interactions based on their inferred impact on target gene expression changes within the recipient cells.

2.7. In vitro dendritic cell culture

Primary mouse peripheral blood mononuclear cells (PBMC) were cultured following a standardized protocol. Initially, a vial containing 1ml of cells was placed into a water bath at approximately 37°C for rapid thawing. Gentle agitation was employed to facilitate the process. Once the ice was nearly dissolved, the vial was removed from the bath. The thawed cells were then transferred using a 1ml pipette from the vial to a 15ml conical tube containing roughly 10ml of base culture media. This mixture was centrifuged at 300g for 5 minutes. The supernatant was aspirated and discarded, and the cell pellet was resuspended in 1.5ml of base culture media. For induction experiments, cells were seeded into a 96-well plate with three repeats per condition. Cells were plated at 10,000 cells per well in comprehensive base media with 5% FLT3L conditioned media. For the IL-4 and mCSF treatment groups, the cytokines were added at concentrations of 10ng/ml or 20ng/ml, respectively. Cells were cultured for 5 days and harvest with cold PBS plus EDTA for flow cytometry.

2.8. Flow cytometry

Cell harvested from *in vitro* culture were prepared for flow cytometry. Samples were blocked with mouse Fc block for 20 min to minimize unspecific bindings. Cells were then stained with a panel of antibodies for 45min, rotating in the dark at 4°C. The antibodies used were: anti-CD45-BUV805, anti-CD3-PE-Fire700, anti-CD11b-BUV737, anti-CD11c-BV711, anti-Ly6c-BV570, anti-CD115-APC, anti-Ly6G-BV650, anti-XCR1-BV421, anti-SIRPa-PE Dazzle 594, anti-MHCII-BUV496. Flow cytometry was performed on a cytek spectrum cytometer and data were analyzed using Flowjo V10. Statistical analysis was performed using Prism.

3. Results

3.1. T cells in ascites having an anti-tumor transcriptional profile compared to tumor compartments

As the direct targets of different immunotherapies, T cells play a crucial role as primary agents in the immune response against tumors, as they selectively identify and respond to antigens expressed by cancer cells. Therefore, a better understanding of tumor-induced T cell profile variations in different tissues is critical in understanding the underlying mechanisms of tumor growth and metastasis and thus is helpful in improving the clinical outcome of patients with cancer.

Through scRNA-seq analysis of T cells drawn in PBMC, ascites, primary tumor, and metastatic tumor of 10 patients, 26 distinct transcriptional clusters were identified (Fig. 1a) with a myeloid cell contamination group in cluster A8. Comparing the blue (PBMC) and red (Ascites) clusters in Fig.1b, we treat cells in PBMC as a control group to eliminate the possibility of potential contamination of the ascites cell profile by blood.

Cluster BAT2 had expression profiles consistent with Teff (high EOMES and CXCR3) [10][11], which were largely anti-tumor. BA6, predominently present in PBMC and ascites, corresponded a robust and typical Teff cell cluster with high cytotoxicity (high expression of CX3CR1, GNLY, ZNF683, TBX21, GZMB, and PRF1) [12]. The two most cytotoxic clusters were dominated by cells from ascites and PBMC. Cluster Ascites13 was potentially repressive due to its high expression level of XCL1 as Tγδ, which could induce pro-tumor immunity by enabling DC1 activation of Treg [13]. Tu7 exhibited high transcripts for negative checkpoint and exhaustion markers that indicate exhaustion (PDCD1, TIGIT, and CTLA4) [12]. Clusters Tu5 and BA14 both displayed characteristics of regulatory T cells, but with higher expression levels of FOXP3 and CCR8, Tregs in Tu5 were more functional and therefore

DOI: 10.54254/2753-8818/59/20241388

immuno-suppressive [14]. Overall, the T cell profiles lean more toward anti-tumor characteristics compared to those observed in tumor tissues.

To further confirm this pattern observed, we focused on CD8+ T cells, the population acknowledged as the most efficacious in tumor immunity, in ascites and tumor. Differentially Expressed Genes (DEGs) between ascites and tumor revealed that CD8+ T cells in ascites were enriched in memory T cell and progenitor exhaustion T cell markers, including TCF7, EOMES, and KLF2 [16]. Previous studies have established that CD8+ T cells expressing these markers promote memory maintenance and respond to immune checkpoint blockade (ICB) [17]. Conversely, those in the tumor exhibited the expression of markers such as NR4A2, NR4A3, and RGS2, associated with TCR signaling and residence (Fig. 2a) [18]. However, it is worth mentioning that the specific impact of these genes characterized in CD8+ T cells would depend on additional factors, including the overall immune microenvironment, the presence of other co-stimulatory or co-inhibitory signals, and the specific signaling pathways involved.

For a more comprehensive overview of the entire transcriptional profile of CD8+ T cells in ascites and tumor, and to evaluate their enrichment in previously published T cell pathways, GSEA analysis was conducted (Fig. 2b). The upregulated genes of CD8+ T cells in ascites versus tumor were significantly enriched in previously published Teff and Tem signatures [19], whereas CD8+ T cell transcription profiles in tumor were characterized as dysfunctional and exhausted [20][21].

GSEA analysis indicated that CD8+ T cells in ascites have potential anti-tumor functions; therefore, we further explored the prognostic values of CD8+ T cell profiles in ascites versus tumor. We grouped 487 Stage III/IV ovarian cancer patients into high or low enrichment of the top 100 upregulated genes in CD8+ T cells from ascites versus tumor, and performed Kaplan-Meier survival analysis. With a hazard ratio of 0.68 and p-value of 0.0013, we concluded that transcriptional profiles of CD8+ T cells in ascites correlated with a more favorable prognosis for metastatic ovarian cancer patients. Besides, despite a p-value of 0.06, a discernible trend suggested that patients with a transcription profile leaning toward CD8+ T cell in the tumor had a lower mean survival rate.

Besides CD8+ T cells, Treg, the primary immunosuppressive population in the tumor microenvironment, also displayed a high heterogeneity in ascites and tumor (Cluster BA14 and Tu5). As a T cell subset pivotal in shaping the balance between anti-tumor immunity and immune tolerance, regulatory T cells held profound implications for cancer prognosis and development. To better understand their heterogeneity and correlation with tumor development, GSEA analysis was applied to elucidate the enrichment of Treg-related pathways (Fig. 2d). The result revealed that Tregs in tumor (Tu5) and ascites (BA14) correspond to KAI_TREG_1 and KAI_TREG_2, respectively, as previously characterized by Luoma et al [15]. KAI_TREG_1 is characteristic of Th1 (IL12RB2, CXCR3, STAT1, TNFRSF18), which are generally considered anti-tumor due to their promotion of cell-mediated immunity and cytotoxic T cell activity, while KAI_TREG_2 is enriched in KLF2, LEF1, and ITGB1, generally associated with Treg regulatory phenotype and suppressive capacity [22].

To further explore the heterogeneity of Tregs in ascites and tumor, their prognostic outcomes were evaluated using survival analysis by grouping 487 Stage III/IV ovarian cancer patients based on high or low enrichment of the top 100 upregulated genes in Treg cells from tumor versus ascites. Kaplan-Meier survival analysis revealed a hazard ratio of 1.5 and a p-value of 0.00067, suggesting that enrichment in Treg signature of Tu5 compared to BA14 was a significant predictor of worse patient overall survival (Fig. 2e).

Overall, these analyses suggested that T cells in ascites own a less exhausted and more memory-like feature, the enrichment of which was associated with better prognosis of metastatic ovarian cancer patients.

DOI: 10.54254/2753-8818/59/20241388

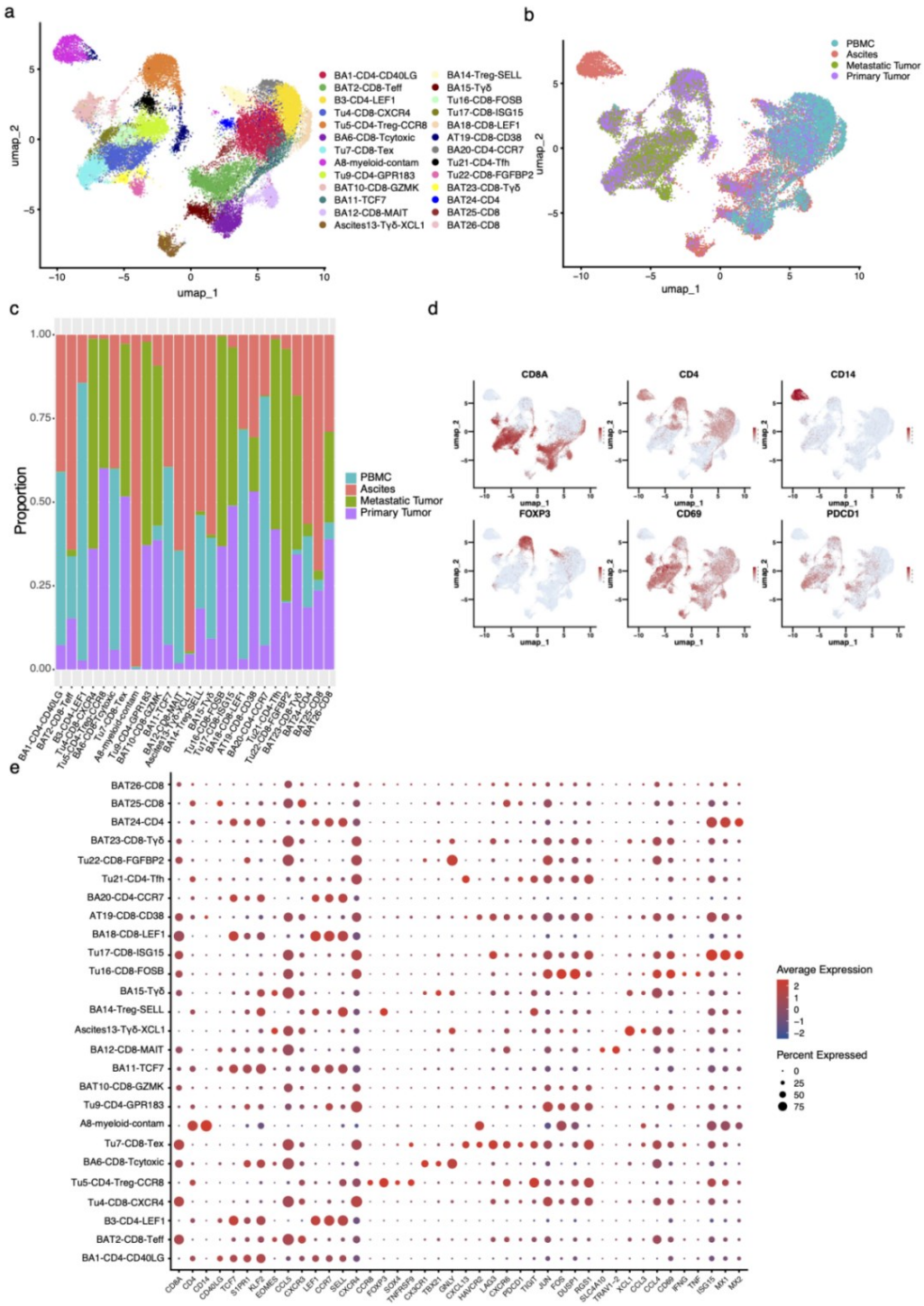

Figure 1. (a) Uniform Manifold Approximation and Projection (UMAP) projection of T cells from PBMC, ascites, primary tumor, and metastatic tumor. Each dot in the visualization represents a single cell with its color reflecting distinct transcriptional profiles. The cells are organized into 26 clusters, each assigned a name based on the predominant tissue (B = PBMC, A = Ascites, T/Tu = Tumor), cell type, and representative markers. **(b)** UMAP projection of T cells, colored based on tissue. **(c)** Stacked bar chart showing the proportion of cells from different tissues in each cluster. **(d)** Feature plots demonstrating the expression of marker genes for CD8+ T-cell (CD8A), CD4+ T-cell (CD4), Treg(FOXP3), T-cell residency (CD69), T-cell exhaustion (PDCD1), and myeloid control (CD14).

DOI: 10.54254/2753-8818/59/20241388

The color scale represents the normalized gene expression level. **(e)** Dot plot showing the transcriptional profile of each cluster. The dot size indicates the percentage of cells expressing the feature within each cluster, while the color reflects the average expression level.

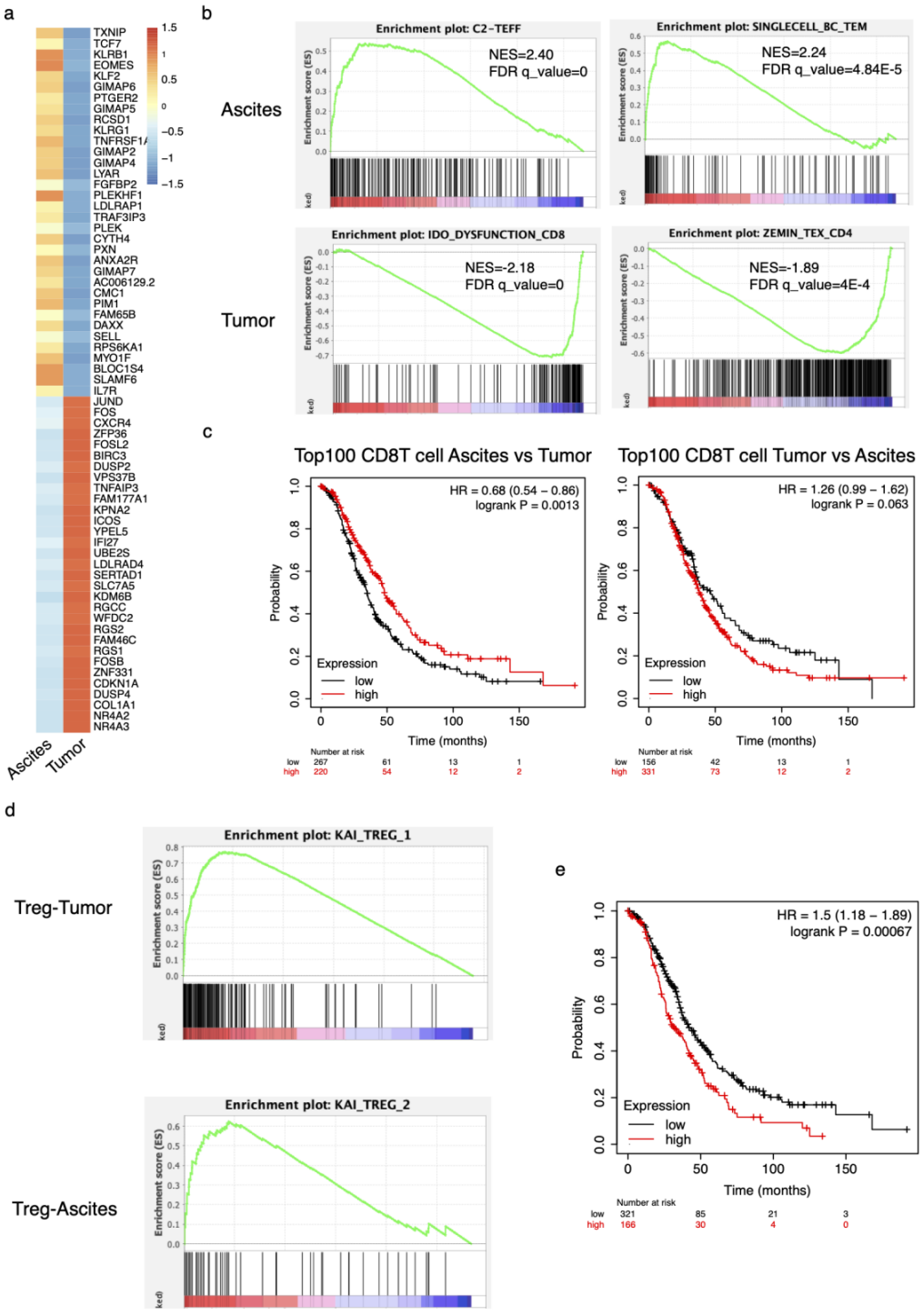

Figure 2. (a) Heatmap showing top differentially-expressed genes between CD8+ T cells in ascites and tumor, colored based on expression level. **(b)** Gene Set Enrichment Analysis (GSEA) indicating that the upregulated genes of CD8+ T cells in ascites and tumor are significantly different. Statistical analysis is conducted utilizing a two-sided permutation test, with multiple testing corrections carried out using the

DOI: 10.54254/2753-8818/59/20241388

BH-FDR method. The results include high Normalized Enrichment Scores (NESs) and low False Discovery Rate (FDR) q-values. **(c)** Kaplan–Meier survival curves of Stage III and IV ovarian cancer patients stratified by enrichment of top 100 signatures of CD8+ T cells in ascites vs. tumor (left) and tumor vs. ascites (right). **(d)** GSEA of CD4 Treg cells in tumor and ascites, enriched in Treg-1 and Treg-2 [15] markers respectively. **(e)** Survival analysis of Stage III and IV ovarian cancer patients stratified by enrichment of top 100 signatures of Treg in tumor vs. ascites.

3.2. Interactions between peritoneal DC populations and CD8+ T cells

Since T cell activation and profiles are highly associated with myeloid cells, especially dendritic cells, our next step was to explore the potential interactions between the peritoneal dendritic cells and T cells in ascites through separating all cells in ascites for scRNA-seq analysis. A total of 26 clusters were identified, including clusters of macrophage, DC, T cells, and B cell (Fig. 3a). Dendritic Cell populations were further divided into 4 subsets including MoDC (CD1c, CD14+), cDC1(XCR1, CD103), cDC2 (CD1c, CD11c), and migratory DC(CCR7, CCL21, CCL19), which were represented in pink, yellow, and purple, respectively. Other myeloid cells such as macrophages were also observed with 6 subsets. Six subsets of T cells were identified: Naive/Central Memory T cell, activated T cell, Tc17, Regulatory T cell, and 2 clusters of effector T cell.

Our previous findings indicate a distinct transcriptional profile of CD8+ T cells in ascites compared to tumors. In light of the understanding that myeloid cells play a pivotal role in regulating T cell function, the previous finding underscores the potential contribution of myeloid cells, especially dendritic cells, to these unique T cell profiles within the ascitic microenvironment. To delve deeper into the intracellular interactions and mechanisms, we performed NicheNet analysis, utilizing activated T cell clusters as receivers and all DC subsets as senders (Fig. 3c). The analysis revealed intricate relationships between DC populations and key transcriptional regulators in T cells. All populations of DC were found to be highly related to MYC in T cells (red), which is a part of the transcriptional network controlling T cell proliferation and differentiation after activation [23]. IL1B and TGFB1 in moDC interact with RORC on CD8+ T cells, a transcription factor regulating the differentiation and function of Tc17 and pathways necessary for cancer metastasis [24]. EOMES, essential for anti-tumor immunity of CD8+ T cells [16], were also observed to be regulated by DC cells, specifically by HLA-A protein on migratory DCs (yellow). As the T cell markers listed in NicheNet analysis were selected to be the top differentially expressed genes in ascites, we can infer that the difference in CD8+ T cell profiles between ascites and tumor were contributed by the T-DC interactions shown on the graph. Overall, ligands of moDC (brown) displayed the most interactions with T cells, while the least signaling pathways were recognized with those of cDC2 (purple).

To discern the relevance of myeloid cell populations, particularly dendritic cells, in the context of clinical prognosis, we delved into a comparative analysis of myeloid cells in ascites and normal adults. There were no observable differences in prevalence and abundance between DCs in the two conditions. The dot plot confirmed this observation, illustrating that there is no significant difference in the proportion of the DC population among all the cells (Fig. 3f). A similar level of enrichment for all DC subsets in ascites patients and normal adults indicated that even though ascites is a worse prognosis factor clinically, peritoneal tumor microenvironment still holds meaningful myeloid cell populations that are essential to T cell activation and activities.

Building on our observation that all four DC populations exhibit extensive characterized cell signaling pathways in interaction with CD8+ T cells, we did a preliminary experiment to establish an *in vitro* culture system from more accessible PBMC, instead of traditional Hematopoietic stem cells (HSCs), to induce different dendritic cells populations.

DOI: 10.54254/2753-8818/59/20241388

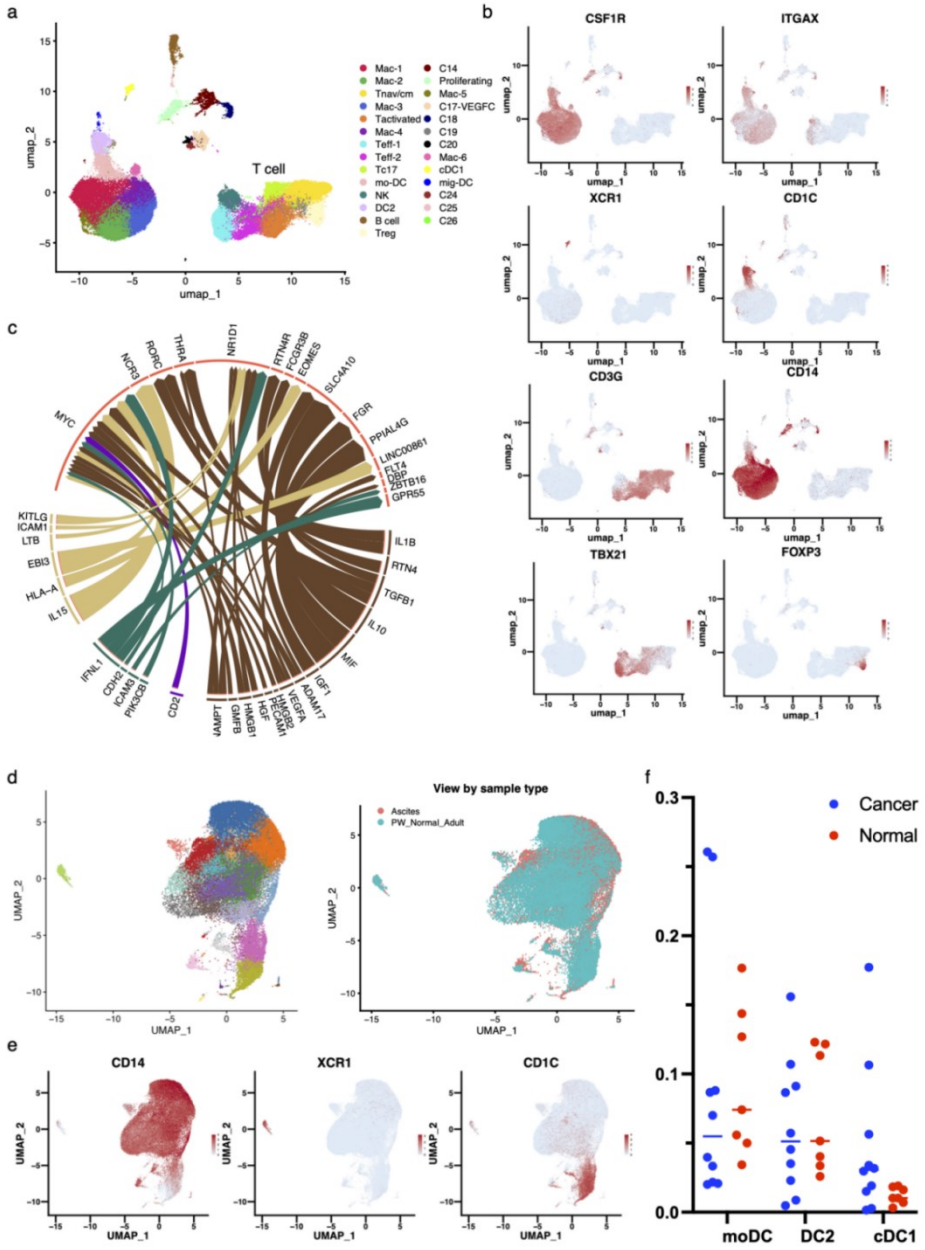

Figure 3. (a) UMAP projection of all cells from ascites of 10 ovarian cancer patients. The cells are organized into 26 clusters, each assigned a name based on the cell type. Myeloid cells (left), T cells (right), and B cells (top) were identified. **(b)** Feature plots demonstrating the expression of marker and subset genes for dendritic cells (ITGAX, XCR1, CD1C, CD14), myeloid cells (CSF1R, CD14), and T cell (CD3G, FOXP3, TBX21). The color scale represents the normalized gene expression level. **(c)** NicheNet analysis utilizing activated T cell clusters as receivers and all DC subsets as senders. All four DC subsets, including moDC (brown), cDC2 (purple), cDC1 (green), and migratory DC (yellow), were found to interact with top differentially expressed genes of CD8 T cells in ascites versus tumor (red). **(d)** UMAP projection of myeloid cells in malignant ascites of ovarian cancer patients and peritoneum of normal adults obtained through peritoneal washing, colored based on cell type (left) and tissue (right). **(e)** Feature plots demonstrating the expression of marker and subset genes for monocytes/moDC (CD14), cDC1 (XCR1), and DC2 (CD1C). **(f)** Dotplot showing the proportion of each dendritic cell population (moDC, DC2, and DC1) in all peritoneal myeloid cells for subjects with (blue) or without (red) cancer. No significant difference between the two conditions are identified.

DOI: 10.54254/2753-8818/59/20241388

3.3. *Experimental Results*

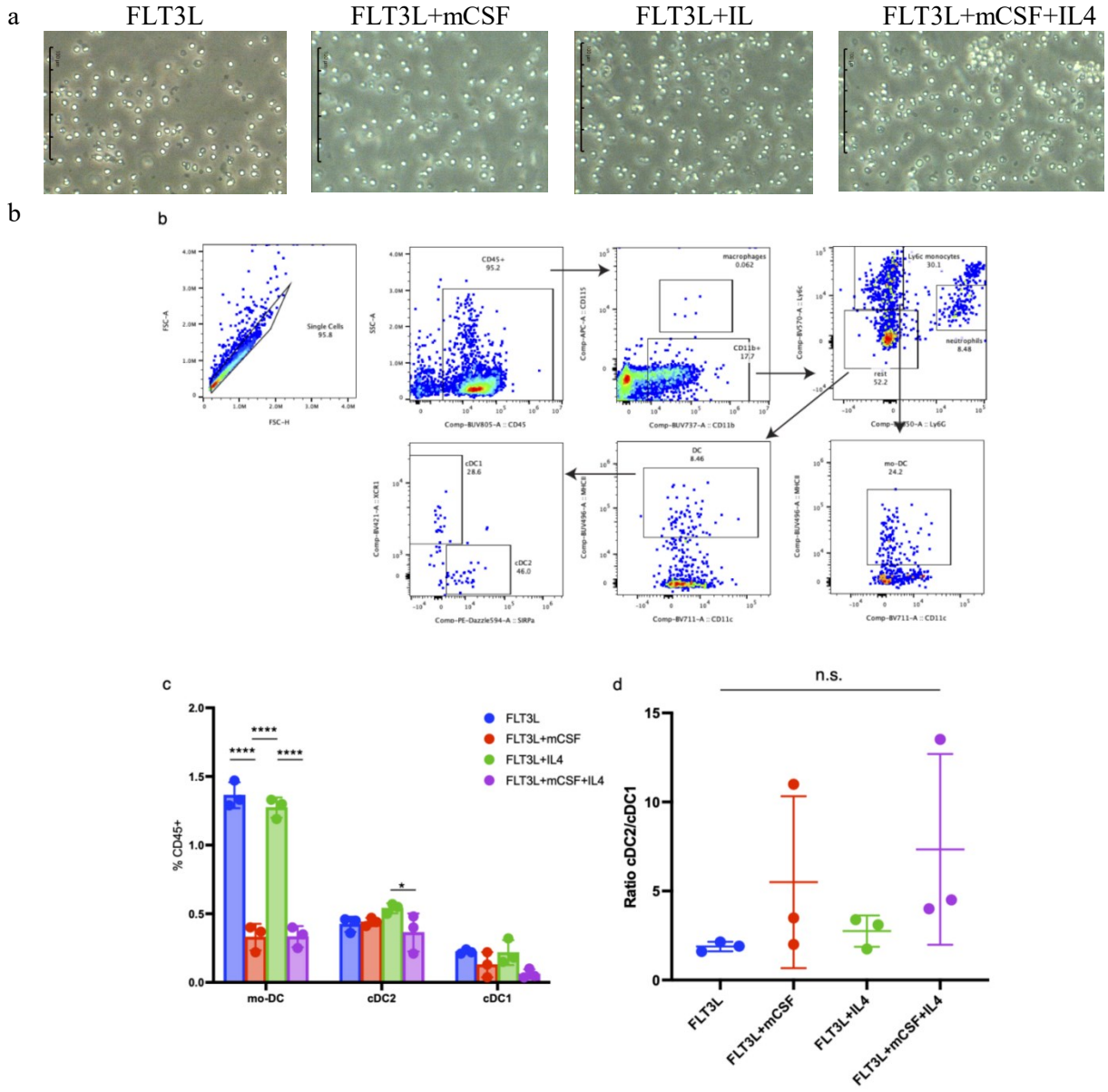

Figure 4. (a) *In vitro* culture of KM mouse PBMC cells within different induction media adding cytokines as specified. **(b)** Representative pseudocolor dot plots showing the gating strategy for DC population in flow cytometry analysis. A density plot of forward scatter height (FSC-H) against forward scatter area (FSC-A) excludes doublets and keeps single cells for further analysis. Two-parameter density plots were then employed to gate leukocytes (CD45+), myeloid cells (CD11b+), Ly6c monocytes (Ly6c+Ly6G-), and distinguish moDC(MHCII+CD11c), cDC1 (XCR1+), and cDC2 (SIRPα+). **(c)** Bar chart showing the distribution and proportions of DC subsets among total myeloid cells across different experimental conditions. The X-axis delineates dendritic cell subset populations, specifically DC1, DC2, and moDC. The Y-axis quantifies the proportion of the specified cell type on the X-axis within the total myeloid cell population. Each bar is distinctly colored to denote the associated treatment group. *P < 0.05; **P < 0.01; ***P < 0.001; t-test corrected for multiple comparison. **(d)** Ratio of the amount of cDC2 over cDC1 from different treatment groups. No significant difference was observed between cell proliferations; t-test corrected for multiple comparison.

DOI: 10.54254/2753-8818/59/20241388

Finally, we explored an *in vitro* platform to culture and expand different subtypes of DCs from PBMC, aiming to help the development of DC vaccines for ovarian cancer patients. PBMC was used instead of the bone marrow due to its accessibility and imposition of less burden on patients in clinical practices. It also promises a more sustainable supply for the development of cancer vaccines, making them a cost-effective and readily available alternative compared to bone marrow. Mouse PBMC was bought from Nexell Life Sciences and the cells were cultured in 96 well plates with a starting number of 10,000 cells/well. Based on the fact that pre-DCs express FLT3, we cultured the cells with FLT3L with or without additional IL-4 and m-CSF.

We successfully expanded cells in all conditions (Fig. 4a) after 5 days of culturing. To determine the phenotypes of cultured cells, we performed multi-color flow cytometry. Markers stained included leucocyte marker CD45, myeloid cell marker CD11b and CD11c, macrophage marker CD115, monocyte marker Ly6c, neutrophil marker Ly6G, cDC1 marker XCR1, cDC2 marker SIRPa as well as MHCII molecules IA/IE (Fig. 4b). A representative plot in Figure 4b demonstrated that we successfully expanded cDC1, cDC2, and mo-DCs *in vitro* from mouse PBMC (Fig. 4b). We further checked the proportions of different subtypes of DCs among all CD45+ populations under different culture conditions and found that FLT3L is sufficient in inducing all subtypes of DCs including mo-DC, cDC1 and cDC2 cells (Fig. 4c). The addition of IL4 did not significantly increase the expansion of mo-DC, cDC1, or cDC2 populations, suggesting that pre-DCs in blood already have a determined differentiation lineage. Interestingly, mCSF induced a decrease in the mo-DC and cDC1 proportions, indicating that mCSF might hinder the differentiation of those populations. Finally, we checked the cDC2 to cDC1 ratios across all conditions to test if different cytokines led to a skewed differentiation (Fig. 4d). Similar to the previous findings, we did not see significant changes in cDC2/cDC1 ratios among different conditions, indicating that IL-4 and mCSF did not determine the differentiation lineage of pre-DCs in PBMC. In all, though further experiments need to be performed to optimize the culturing protocols to better expand the DC populations as well as examine the function of the cultured DC subsets, here we proved the potential of using an *in vitro* culturing system to expand different populations of DC subsets through different inducing media from PBMCs for potential cancer vaccines designs.

4. Discussion

This study advanced our understanding of the complex landscape of T cell heterogeneity in the tumor microenvironment (TME) and its surrounding tissues, employing single-cell RNA sequencing (scRNA-seq) to identify 26 distinct transcriptional clusters across peripheral blood mononuclear cells (PBMCs), ascites, primary tumors, and metastatic tumors. Our findings underscore the nuanced associations between T cell subsets and the TME, highlighting potential pathways for enhancing immunotherapy efficacy.

The identification of distinct T cell clusters with varied transcriptional profiles, especially those associated with effector functions (e.g., clusters BAT2 and BA6), regulatory mechanisms (clusters Tu5 and BA14), and tissue residency (cluster B3 and Tu16), underscores the intricate balance between anti-tumor immunity and immune evasion mechanisms within the TME. Notably, the comparison of T cells from ascites and PBMCs revealed significant differences in their transcriptional landscapes, pointing towards a unique immune microenvironment in the peritoneal cavity that could influence tumor progression and response to therapy.

Our analysis revealed that T cells within ascites tend to display less exhaustion and possess more memory-like features compared to their counterparts in tumor tissues. This observation is particularly relevant for immunotherapy strategies, as memory T cells are known for their long-lived and robust response to antigen re-exposure. The enrichment of CD8+ T cells in ascites, amidst immunosuppressive pressure, with markers indicative of memory and progenitor exhaustion states (e.g., TCF7, EOMES, and KLF2) suggests a potential for these cells to be leveraged in immunotherapeutic approaches aiming to enhance the durability and effectiveness of anti-tumor responses.

Furthermore, the differential expression of genes associated with T cell exhaustion and activation between ascites and tumor-resident T cells provides valuable insights into the mechanisms driving T

DOI: 10.54254/2753-8818/59/20241388

cell dysfunction within the TME. The presence of clusters with high expression of exhaustion markers (e.g., PDCD1, CTLA4, TIGIT) in tumor tissues reflects the immunosuppressive nature of the TME and highlights the need for strategies that can reinvigorate these exhausted T cells.

The interaction between T cells and dendritic cells (DCs) in ascites, as indicated by our NicheNet analysis, further emphasizes the role of myeloid cells in shaping T cell responses within the TME. The engagement between moDC-derived ligands and T cell receptors underscores the potential for modulating DC-T cell interactions to enhance anti-tumor immunity. This aspect of our findings points towards the importance of understanding the cross-talk between different immune cell types in the TME, which could inform the development of combination therapies that target multiple facets of the immune response.

Additionally, our survival analysis based on the transcriptional profiles of CD8+ T cells and regulatory T cells (Tregs) in ascites versus tumor tissues provides a prognostic perspective, linking the immunological characteristics of the TME with clinical outcomes. The association between the transcriptional signature of ascites-resident CD8+ T cells and improved patient prognosis underscores the therapeutic potential of harnessing these cells to combat tumor progression.

Despite these insights, questions remain regarding mechanisms governing differential T cell polarization in ascites versus tumors. Future in-depth functional validations should investigate specific pathways driving exhaustion versus memory and effector signatures across sites. Additionally, while our development of the *in vitro* platform to induce DC populations is a step forward, further investigations including skewing DC transcriptional profiles and co-culture of dendritic cells and T cells are meaningful in further addressing the intricacies of dendritic cell functionality and proving the cause-and-effect relationship between DC population and T cell behavior. Furthermore, comparisons of matched primary carcinomas, metastases, and ascites from more patients are needed to confirm the broader clinical applicability of our conclusions about relative T cell potency across anatomic compartments.

In summary, our study provides a comprehensive atlas of T cell heterogeneity within and around the tumor microenvironment, highlighting the dynamic interplay between immune cell subsets and the TME. These insights pave the way for the development of more nuanced immunotherapeutic strategies that consider the spatial and functional diversity of T cells in cancer. As we continue to unravel the complexities of the immune landscape in cancer, future research should focus on translating these findings into clinical applications, potentially through the design of targeted therapies and vaccines that can modulate the immune response to achieve durable anti-tumor effects.

5. Conclusion

This study uncovered a distinct transcriptional profile in T cells found in ascites in contrast to those found within tumors. This profile shows promise as a prognostic indicator and is largely shaped by all subsets of dendritic cells present in ascites. Delving into the immune landscape of ovarian cancer (OC), the study sheds light on the previously understudied realm of malignant ascites during peritoneal metastasis. While OC immune analyses conventionally focus on solid tumors, our exploration of the single-cell landscape in malignant ascites provides a novel perspective. The identification of less exhausted and more memory-like T cells within ascites, contrasting with the immunosuppressed tumor environment, holds profound clinical implications. This T cell profile in ascites also correlates with prolonged survival in stages III/IV OC patients, emphasizing the potential prognostic significance of ascites immune cells. Moreover, our characterization of the interactions between dendritic cells and T cells in ascites provides an insight into the intricate dynamics contributing to the unique T cell ecosystem within the ascites microenvironment. Additionally, the exploration of an *in vitro* dendritic cell culture system from PBMC paves the way for future studies to skew DC subset population and further characterize DC-T interaction through co-culturing DC and T cells. This study not only advances our understanding of OC immunity but also underscores the importance of considering ascites microenvironment as a crucial component in exploring the immune responses in ovarian cancer. The

DOI: 10.54254/2753-8818/59/20241388

results lays the foundation for future immunotherapeutic strategies that target the specific immune landscape in ascites.

References

[1] Cancer today. http://gco.iarc.fr/today/home.

[2] Gaitskell, K. *et al.* Ovarian cancer survival by stage, histotype, and pre-diagnostic lifestyle factors, in the prospective UK Million Women Study. *Cancer Epidemiol.* 76, 102074 (2022).

[3] Larkin, J. *et al.* Five-Year Survival with Combined Nivolumab and Ipilimumab in Advanced Melanoma. *N. Engl. J. Med.* 381, 1535–1546 (2019).

[4] Bai, R. *et al.* Mechanisms of Cancer Resistance to Immunotherapy. *Front. Oncol.* 10, 1290 (2020).

[5] Liu, M., Silva-Sanchez, A., Randall, T. D. & Meza-Perez, S. Specialized immune responses in the peritoneal cavity and omentum. *J. Leukoc. Biol.* 109, 717–729 (2021).

[6] Blank, C. U. *et al.* Defining 'T cell exhaustion'. *Nat. Rev. Immunol.* 19, 665–674 (2019).

[7] Corthay, A. How do Regulatory T Cells Work? *Scand. J. Immunol.* 70, 326–336 (2009).

[8] Backer, R., Probst, H. & Clausen, B. Classical DC2 subsets and monocyte-derived DC: Delineating the developmental and functional relationship. *Eur. J. Immunol.* 53, (2023).

[9] Zheng, X. *et al.* Single-cell analyses implicate ascites in remodeling the ecosystems of primary and metastatic tumors in ovarian cancer. *Nat. Cancer* 4, 1138–1156 (2023).

[10] Kurachi, M. *et al.* Chemokine receptor CXCR3 facilitates CD8+ T cell differentiation into short-lived effector cells leading to memory degeneration. *J. Exp. Med.* 208, 1605–1620 (2011).

[11] Li, J., He, Y., Hao, J., Ni, L. & Dong, C. High Levels of Eomes Promote Exhaustion of Anti-tumor CD8+ T Cells. *Front. Immunol.* 9, (2018).

[12] van der Leun, A. M., Thommen, D. S. & Schumacher, T. N. CD8+ T cell states in human cancer: insights from single-cell analysis. *Nat. Rev. Cancer* 20, 218–232 (2020).

[13] Rezende, R. M. *et al.* γδ T Cell-Secreted XCL1 Mediates Anti-CD3-Induced Oral Tolerance. *J. Immunol. Baltim. Md 1950* 203, 2621–2629 (2019).

[14] Barsheshet, Y. *et al.* CCR8+FOXp3+ Treg cells as master drivers of immune regulation. *Proc. Natl. Acad. Sci. U. S. A.* 114, 6086–6091 (2017).

[15] Luoma, A. M. *et al.* Molecular Pathways of Colon Inflammation Induced by Cancer Immunotherapy. *Cell* 182, 655-671.e22 (2020).

[16] Llaó-Cid, L. *et al.* EOMES is essential for antitumor activity of CD8+ T cells in chronic lymphocytic leukemia. *Leukemia* 35, 3152–3162 (2021).

[17] Chen, Y., Zander, R., Khatun, A., Schauder, D. M. & Cui, W. Transcriptional and Epigenetic Regulation of Effector and Memory CD8 T Cell Differentiation. *Front. Immunol.* 9, 2826 (2018).

[18] Boelte, K. C. *et al.* Rgs2 Mediates Pro-Angiogenic Function of Myeloid Derived Suppressor Cells in the Tumor Microenvironment via Upregulation of MCP-1. *PLoS ONE* 6, e18534 (2011).

[19] Han, J. *et al.* Resident and circulating memory T cells persist for years in melanoma patients with durable responses to immunotherapy. *Nat. Cancer* 2, 300–311 (2021).

[20] Guo, X. *et al.* Global characterization of T cells in non-small-cell lung cancer by single-cell sequencing. *Nat. Med.* 24, 978–985 (2018).

[21] Li, H. *et al.* Dysfunctional CD8 T Cells Form a Proliferative, Dynamically Regulated Compartment within Human Melanoma. *Cell* 176, 775-789.e18 (2019).

[22] TCF1 and LEF1 Control Treg Competitive Survival and Tfr Development to Prevent Autoimmune Diseases - PubMed. https://pubmed.ncbi.nlm.nih.gov/31216480/.

[23] Gnanaprakasam, J. N. R. & Wang, R. MYC in Regulating Immunity: Metabolism and Beyond. *Genes* 8, 88 (2017).

[24] Oh, T. G. *et al.* The Nuclear Receptor, RORγ, Regulates Pathways Necessary for Breast Cancer Metastasis. *EBioMedicine* 6, 59–72 (2016).